

HST Spectroscopy of the Nucleus of M33¹

Knox S. Long

*Space Telescope Science Institute,
3700 San Martin Drive, Baltimore, MD 21218*

Philip A. Charles

*Department of Physics & Astronomy,
University of Southampton,
Southampton SO17 1BJ, UK*

and

Guillaume Dubus

*California Institute of Technology, Mail Code 130-33
Pasadena, CA 91125*

ABSTRACT

We have used Hubble Space Telescope to obtain moderate resolution 1150-5700 Å spectroscopy of the nucleus of M33 and a blue star ~ 1 arcsec NNW of the nucleus in an attempt to find the optical counterpart of the nuclear X-ray source and to characterize stellar populations in the nuclear region. The STIS spectra of the nucleus can be modelled in terms of two starbursts, one with a mass of about 9000 M_{\odot} at 40 Myrs and the other with a mass of about 76,000 M_{\odot} at 1 Gyrs. The blue star is a late type O giant, with no obvious spectral anomalies to indicate that it is associated with the luminous X-ray source. The nuclear region is not heavily reddened; 2200 Å absorption features in the spectra of both the nucleus and the star are weak. The data and the star formation history support the hypothesis that the M33 nuclear source, the brightest persistent source in the Local group, is an $\sim 10 M_{\odot}$ black hole binary.

Subject Headings: galaxies: individual (M33)galaxies: nucleiLocal Groupultraviolet: stars galaxies : stellar content

¹Based on observations made with the NASA/ESA Hubble Space Telescope, obtained at the Space Telescope Science Institute, which is operated by the Association of Universities for Research in Astronomy, Inc., under NASA contract NAS 5-26555. These observations are associated with proposal # 8341.

1. Introduction

The nucleus of M33 houses the most luminous persistent X-ray source in the Local Group (Long et al. 1981; Markert & Rallis 1983; Long et al. 1996). The nuclear X-ray source is about 8 times brighter than any other X-ray source in M33, and significantly brighter than any source in the nuclear region of M31 (Supper et al. 2001). That the brightest source in the Local Group would be located in the nucleus of M33 was, and remains, surprising because there is no evidence that M33 contains a large central mass concentration (Kormendy & McClure 1993; Merritt, Ferrarese, & Joseph 2001; Gebhardt et al. 2001).

Since visible light from the nucleus of M33 is most likely dominated by late type stars, searches for the optical counterpart to the X-ray source seem most likely to succeed at UV wavelengths. To test this idea, (Dubus, Long, & Charles 1999, hereafter DLC) imaged the nuclear region of M33 with HST. These observations showed that in the UV, the nucleus is both brighter than expected from its optical color temperature and more compact than at long wavelengths, as might be expected if one were observing the accretion disk of a compact binary X-ray source. About half of the total UV luminosity of 3×10^{38} ergs s⁻¹ comes from the inner 0.14 arcsec. However, because the angular size of the nucleus is relatively close to the limiting angular resolution of HST, it was not possible to determine whether the emission observed at the center is from a true point source or simply a more concentrated, bluer stellar population (see also Lauer et al. 1998; Matthews et al. 1999).

O’Connell (1983) made one of the first attempts to understand the stellar population history of the M33 nucleus partly in response to the discovery of the nuclear X-ray source. While the appearance and mass of the nucleus resembles a globular cluster in some ways, he concluded that about 50% of the visible light from the nucleus arises from stars of <1 Gyr in age, and that the youngest stars are likely to have been formed about 50 Myrs ago. Most subsequent studies have added credence to this suggestion. For example, Schmidt, Bica, & Alloin (1990) found that the visible UV portion of the spectrum is dominated by a near solar abundance population of stars aged less than 500 Myrs, while at longer wavelengths an intermediate and then older populations become progressively more important. More recently Gordon et al. (1999), modelling both broad band photometry from FUV to NIR wavelengths, as well as optical and NIR spectra of M33, have suggested that nearly all of the light arises from a burst of star formation 70 Myrs ago “enshrouded by a shell of MW-style dust with $\tau_\nu \sim 2$ ”.

In an attempt to identify the optical counterpart to the bright nuclear source in M33 and also to better characterize the source populations in the nucleus of M33, we have now carried out spectroscopic observations of the nucleus using the Space Telescope Imaging Spectrograph on HST (Woodgate et al. 1998) covering the wavelength range 1150 - 5700 Å.

The remainder of this paper describes the results of this investigation.

2. Observations

The STIS observations of the nucleus of M33 are summarized in Table 1. As indicated, the spectra were acquired in two “visits”, one lasting 4 orbits in 1999 October, covering the FUV (1150-1730 Å), and the other a year later lasting 2 orbits, covering the NUV (1570-3180 Å) and “visible” (2900-5700 Å). These gratings were selected to cover the full wavelength range with moderate resolving power (500-1400 depending on wavelength), sufficient to resolve broad lines that might be expected if the nucleus housed a mini-AGN or stars with strong P Cygni profiles and to perform stellar population synthesis. All of the observations were carried out with the 0.1” x 52” slit in order to isolate as much as possible the point source in the nucleus. The orientation of the slit was carefully set so that spectra were obtained of not only the nucleus, but also a 19th magnitude star NNW of the nucleus. This was the only source, other than the nucleus, detected within a few arcsec of the nucleus in the 1600 Å (F160BW) image. (See Figure 1 of DLC.) The acquisition images indicate that the slit was accurately centered on the nucleus for both observations. From 2 to 8 spectra were obtained at each grating setting; none shows evidence of any temporal variability. In short, all of the observations appear to have been nominal.

All of the observations described here were processed using the standard STIS pipeline and calibration files available in 2000 December. Spectra of the nucleus and the star were extracted from the individual exposures and combined to produce overall spectra shown in Figures 1 and 2. The spectra from the different grating settings appear well-matched where they overlap.

The F_λ spectrum of the nucleus peaks in the UV, and shows a prominent Lyman α absorption profile and narrow absorption lines from a variety of ions including C II, III, and IV, Si II, III, and IV, and Mg II. The Balmer jump is well defined, as had been expected from ground-based observations. But there is no evidence either of wind-features (P Cygni profiles) in the spectra, nor is there evidence of obvious dust absorption in the form of a 2200 Å absorption dip. The spectrum contradicts the suggestion by Gordon et al. (1999), based on assembling a broad-band spectrum from UIT and HST imaging data, that a strong 2200 Å feature is evident in the light of the nucleus.

The spectrum of the star is much bluer than that of the nucleus. The low ionization state lines in the spectrum, Si II, C II λ 1334, and Mg II have similar strengths and widths to those in the nuclear spectrum, suggesting they are predominantly interstellar in both

spectra. On the other hand, the highest ionization state lines, N V $\lambda\lambda 1239, 1243$, Si IV $\lambda\lambda 1394, 1403$, and C IV $\lambda\lambda 1548, 1551$, all show P Cygni profiles, indicating that the star has a massive wind.

In the spectra shown in Figures 1 and 2, the standard extraction widths were used (0.26 arcsec for the FUV and NUV spectra and 0.35 arcsec for the “visible” spectra). An examination of the profiles of the nucleus and the star along the slit shows that the nucleus is extended compared to the star, as was anticipated. (Unfortunately the nucleus is not sufficiently extended to easily extract multiple spectra of the nucleus along the slit.) The flux from the nucleus observed through the 0.1” slit is considerably less than the flux estimated for the entire nucleus from the broad band filters on WFPC2 (see, e.g. Gordon et al. 1999, DLC). The ratio of flux varies from 1/3 at 1600 Å to 1/5 at 5500 Å. In contrast, the STIS fluxes for the star agree within 25% of the broad band fluxes reported by DLC, and there is no obvious trend with increasing wavelength. While it is worthwhile to ask whether this is evidence for variability in the nucleus, we view this as very unlikely. In fact, the fluxes that we observe with STIS are fully consistent with the results of DLC and other investigators showing that $\sim 50\%$ of the UV flux arises within 0.14” of the center of the nucleus and that the size grows at longer wavelengths. We have also extracted spectra of the nucleus using extraction boxes which are somewhat larger than those provided by the STSDAS pipeline. The flux is somewhat (10%) larger at all wavelengths. Given that the nucleus is somewhat less concentrated at longer wavelengths, one might have expected some change in the spectral shape using larger apertures. However, there is little, if any, change observed, and therefore we have used the standard extractions in the analysis which follows.

3. Analysis

The spectra of both the nucleus and the star lack dramatic features in the UV to make identification of the source of X-rays from the nuclear region obvious. However, to understand whether there are more subtle features that signify the optical counterpart to the X-ray emission, a more detailed analysis is required.

3.1. Stellar Synthesis of the Nucleus

Our STIS spectra comprise the first high quality UV spectra of the nucleus of M33. In an attempt to model the spectra we have made use of models generated with Starburst99 (Leitherer et al. 1999). In this initial reconnaissance, we have concentrated on the overall

shape of the spectrum. We have primarily considered models consisting of one or two bursts of star formation, although we also looked at models of continuous starbursts. We have considered models with a Salpeter initial mass function and upper mass cutoffs $100 M_{\odot}$ and $30 M_{\odot}$. Within the context of Starburst99, we have considered models in which the metallicities used to evolve the stellar populations range from 0.001 to 0.08. Comparisons of the models to the data were made using χ^2 minimization routines. Our approach was to begin with pre-calculated models that are available from the Starview99 web site and to use the results as guidance for calculating new models with the version of the software and associated data available in the spring of 2001. Starburst99 produces two sets of spectra, one with relatively modest resolution of $\sim 10 \text{ \AA}$ covering a wide wavelength range, and one with a resolution of 0.75 \AA covering the range 1205-1850 \AA . The first set of spectra are generated with abundances that are based on model atmospheres and are matched to that of the stellar evolution synthesis; the second are based on the observed spectra of stars and are available only for solar and LMC-like abundances. Except where noted we have used the coarser spectra in the discussion which follows. Because the spectra have relatively high S/N, we did not anticipate that χ^2 minimization would allow a strict statistical comparison of the data or evaluation of the errors associated with any particular model. However, it does provide a means for finding the best parameters for a particular model, and a qualitative measure of the degree to which the model approximates the data.

We began with a consideration of single bursts or continuous star formation, and attempted to fit all the data from 1200-5600 \AA using the pre-calculated models, the coarser wavelength model spectra, and a Galactic extinction law, specifically that of Seaton (1979). However this combination never produces qualitatively good fits to the data. The “best fit” was a low-metallicity ($z=0.004$) instantaneous starburst model with an age of 163 Myrs and an $E(B-V)$ of 0.23. In model fitting of this type, the procedure selects parameters, an age, a normalization, and the reddening, that match the continuum, including in this case the Balmer jump. Indeed, the model approximates the spectrum longward of 3000 \AA fairly well, and also produces approximately the correct flux in the FUV region. The narrow lines, including the Balmer lines, are not reproduced, but this is directly attributable to the spectral resolution of the models. As shown in Figure 3, the basic problem with this (and all other simple models using a Galactic absorption law) is the absence, or near absence, of a 2200 \AA absorption feature in the data. It is primarily this feature that results in a χ^2_{ν} of 17.8.

Galactic absorption along the line of sight to M33 is thought to be relatively small ($E(B-V) \sim 0.07$; van den Bergh 1991), and there is no guarantee, or possibly even expectation, that the absorption law in M33 has a 2200 \AA feature as prominent as that represented by a Seaton law with $E(B-V)$ of 0.23. Differences in the absorption law arise both from differences in the grain size distribution, and in extended sources from scattering and multiple optical depths

within the source itself (Calzetti, Kinney, & Storchi-Bergmann 1994). Therefore we have considered two other absorption laws, neither of which exhibits a significant 2200 Å bump. The first of these extinction laws is that proposed by Calzetti, Kinney, & Storchi-Bergmann (1994). This extinction curve was developed to account for the fact that the 2200 Å feature is missing from the UV spectra of many starburst galaxies, even though there is ample evidence for absorption from emission line ratios. The second is for the Small Magellanic Cloud, long known to have a smooth, but highly absorptive UV extinction curve. Here we use the average parameters derived by Gordon & Clayton (1998) for the bar of the SMC .

Allowing for all three extinction laws, the best-fit single component model was the same $z=0.004$ instantaneous starburst model, with a very similar age 143 Myrs, and a Calzetti, or starburst, absorption law with $E(B-V)$ of 0.22. The fit is insensitive to the mass cutoff of 30 or 100 M_{\odot} , but models based on evolutionary tracks for higher metallicity stars result in higher χ_{ν}^2 . An instantaneous burst is better than any of the simple continuous star formation models we tried. As shown in Figure 3, the model fit is greatly improved with a good match to the spectrum longward of 2300 Å, and relatively good approximation to the broad band FUV continuum. The value of χ_{ν}^2 improves to 13.4, reflecting the higher quality of the overall fit. The main problem qualitatively is the structure of the spectrum shortward of 2000 Å, which is smoother in the model than in the observed spectrum. Simple fits made with an SMC-like absorption curve were generally poorer than those made with a starburst absorption law, often worse in fact than those made with a Galactic curve. The underlying reason for this appears to be associated with the fact that the UV absorption is so strong that very low values of $E(B-V)$ result from the model fits, but this results in a spectral slope in the NUV and visible that does not match the data.

The quality of the fit can be improved significantly by allowing for two distinct bursts. The best fit model in this case is a model synthesized from solar abundance ($z=0.02$) tracks and a starburst absorption law with $E(B-V)$ of 0.06. A relatively recent starburst aged 70 Myrs dominates the UV light and competes with an older burst aged 1.1 Gyrs at visible wavelengths. The improvement in the fit to χ_{ν}^2 of 11.9 reflects primarily a better approximation of the model to the FUV portion of the spectrum. The reason that the spectrum is better approximated in the FUV compared to the single starburst model can be traced directly to the spectra of the higher mass stars in a younger starburst. Two component models using either a Galactic ($\chi_{\nu}^2 = 13.8$) or an SMC ($\chi_{\nu}^2 = 12.3$) curve yield similar parameters. But a 2200 Å problem is evident in the fits using a Galactic absorption curve.

We have also experimented with models with three separate components. None of these models improved the fits significantly in a qualitative or quantitative way and all indicated that the youngest stellar component had an age of 40-60 Myrs.

Since the two-component models described above seem to favor models with abundances that are close to solar, we then considered models in which the higher resolution UV stellar spectra were substituted for the coarser model-atmospheres generated spectra in the UV. The best fit two component model has a starburst absorption law with $E(B-V)$ of 0.06, a recent starburst of 50 Myrs and an older one of 1 Gyrs. The value of χ_ν^2 drops to 9.1. Qualitatively, the fit is quite good as indicated in Figure 4. The improvement in χ_ν^2 is clearly due to the incorporation of higher resolution, observation-based data in the UV range. Most of the improvement in χ_ν^2 is due to spectral resolution, although some appears due to differences between the model-based and observation-based stellar spectra that were used to synthesize the nuclear spectrum models. (In fact, we have conducted experiments in which we have resampled the data on the wavelength grid of the models, and then attempted to fit the original data using the resampled data as the “model”. The χ_ν^2 that results is of about 8.)

One of the remaining systematic departures now appears at between 2000 and 2400 Å, where the model and data are discrepant at a level of about 10% of the continuum. This can be eliminated if we allow for Galactic absorption with $E(B-V)$ of 0.07 (van den Bergh 1991). In that case, we find the age of the more recent starburst drops to 40 Myrs, while the older populations is characterized by an age of 1 Gyr, and χ_ν^2 of 9.0. The M33 reddening, parameterized in terms of a starburst absorption curve, remains small, but is actually somewhat higher $E(B-V)=0.11$ than in the case in which Galactic reddening is ignored. As shown in figure 5, there are no large departures between the model and the data that cannot be directly attributed either to the interstellar lines, e.g. Mg II, which are not part of the model, or the coarseness of resolution of the model spectra. In these final fits, about 10% of the mass of the nucleus would have been involved in the recent starburst. The masses required in the 10 Myr and 1.1 Gyr starbursts are about 9000 M_\odot and 76,000 M_\odot .

To summarize, our analysis implies that there are at least two stellar populations in the nucleus and that the younger of these has an age of 40-50 Myrs. The younger population completely dominates the FUV light from the nucleus of M33 and contributes almost half the visible light from the (central part of the) nucleus. This analysis therefore generally confirms those of O’Connell (1983) and Schmidt, Bica, & Alloin (1990) based on optical spectra and limited UV data.

There is no need, based on the HST spectra, to invoke a large amount of internal reddening in the nucleus, as suggested by Gordon et al. (1999). This is not quite the same, however, as proving that there is no M33 reddening, since the our best-fit model using a starburst absorption law suggests that only 38% and 66% of the light emitted at 2000 and 5700) Å emerges from M33. If the absorption is between the nucleus of M33 and ourselves, the implied optical depth is less than 1 at 2000 Å and 0.4 at 5700 Å. But if the the absorption

is within the nucleus itself then the optical depth through the entire nucleus can approach 1 at visible wavelengths.

The stellar population history of the region surrounding the nucleus of M33 is complex, as evidenced by the studies of Minniti, Olszewski, & Rieke (1993) and Mighell & Rich (1995). There are OB associations with ages of about 5 Myrs, a group of luminous AGB stars formed of order 1 Gyrs ago, as well as a considerably older (>10 Gyr) metal poor population. Schmidt, Bica, & Alloin (1990) argued for three similar populations in the nucleus, one aged less than 5 Myrs, a second 1-5 Gyrs, and a third >10 Gyrs, and so it is possible, perhaps likely, that there is a close connection between the history of the the nucleus and the nuclear region. But definitive proof of that assertion will likely require a more sophisticated modelling of the HST spectra than in our first reconnaissance, with stellar models constructed at the resolution of the HST data and probably the inclusion of comparable quality data of the nucleus at longer wavelengths.

3.2. Classification of the Blue Star

The nature of the star NNW of the nucleus is important for our purposes because the astrometric accuracy of all X-ray telescopes, with the possible exception of Chandra, is not sufficient to distinguish a nuclear source and a source 1 arcsec away. Indeed most if not all X-ray imaging surveys of M33 have used the nuclear X-ray source to register the other sources in the field.

In an attempt to establish the spectral type of the star near the nucleus of M33, we first compared the UV spectrum to those found in IUE spectral atlases of O and B stars (Walborn, Nichols-Bohlin, & Panek 1985; Walborn, Parker, & Nichols 1995). These visual comparisons suggest a spectral classification between O8 and B0. Stars of spectral type earlier than O8 show much more prominent N V and Si IV profiles that are very different in strength from those observed in the star in M33. Stars later than B0 have weaker line profiles than is observed in the M33 star. Assuming a spectral type of B0, a luminosity class between II and III was indicated, based on the IUE spectra of HD43818 and HD48434. Main sequence stars have lines that are generally narrower than those observed in our star. Similar results are obtained from a comparison to the atlas used by Leitherer et al. (1999) for spectral synthesis. As indicated in Figure 6, which is a comparison between the reference spectral template for an O9 III, the UV spectrum of the star is not unusual for a late type O giant.

Massey et al. (1996) used the Ultraviolet Imaging Telescope (UIT) on the Astro-2 space

shuttle mission along with ground-based and HST observations to construct a catalog of 356 sources in M33 that is thought to be complete to F_λ of 2.5×10^{-15} ergs cm $^{-2}$ s $^{-1}$ Å $^{-1}$, about 3 times that of the star in M33. (Given that our star is about 3 times fainter than the completeness limit and that the angular resolution of UIT was several arcsec, it is not surprising that our star is not in that catalog.) There are no late O or early B giants in this survey; the 5 O9-B0 supergiants have visual magnitudes that range from 16.8-18.2, which should be compared to the visual magnitude of our star of 19.25 from our earlier HST imaging observations or 19.45 from these STIS observations. The magnitude difference is roughly that expected for a late O or very early B giant (II-III). Equivalently, the absolute visual magnitude (ignoring reddening) of ~ 5.2 , given a distance modulus of 24.5 ± 0.2 (van den Bergh 1991), is consistent with a late O or very early B giant (see, e.g. Allen 1973). Thus we can be reasonably confident of the classification of the star.

4. Discussion

Our initial impulse to obtain a spectrum of the nucleus was motivated by a desire to identify the optical counterpart to the X-ray source in M33. Neither the spectrum of the nucleus nor, for that matter, the spectrum of the nearby star show direct indication of X-ray activity.

A number of suggestions have been made over the years as to the nature of the X-ray source at the heart of M33. These have included a very low luminosity active galaxy, collections of neutron star binaries with high or low mass companions (Markert & Rallis 1983; O’Connell 1983), and, more recently, a binary star system containing an Eddington-limited $10 M_\odot$ black hole (Takano et al. 1994). This last explanation is clearly the favored explanation today as more point-like, super-Eddington sources have been found in and out of the nuclei of normal galaxies (see, e.g. Makishima et al. 2000), since they were originally noted by Long & van Speybroeck (1983). The X-ray spectrum of the M33 source is similar to these other sources.

4.1. A mini-AGN?

Despite recent suggestions of a jet emerging from the nucleus of M33 (Matthews et al. 1999)², the existence of mini-AGN such as NGC4395 (a Sd galaxy with a Seyfert nucleus with an L_X of 10^{38} ergs s^{-1} ; Lira et al. 1999), and clear evidence of a supermassive black hole (SMBH) at the center of our Galaxy, there is little to support a mini-quasar interpretation of M33 X-8:

(1) There is no indication whatsoever of AGN-like activity in our FUV spectra. There is no evidence of broad emission lines, nor for any blue bump which one might associate with the accretion disk. Based on the observed X-ray flux (7.6×10^{-12} erg cm^{-2} s^{-1} keV $^{-1}$ in the 0.1–2.4 keV band; Long et al 1996), we would expect a far-UV flux of $\sim 1 - 6 \times 10^{-15}$ erg cm^{-2} s^{-1} Å $^{-1}$ for an assumed X-ray/optical spectral slopes α_{ox} of 0.65–1 (Wilkes & Elvis 1987). This would represent a significant fraction of the observed flux and yet the UV spectrum is entirely consistent with that of normal early-type stars. Values of α_{ox} in this range would be expected from a direct extrapolation of the X-ray-derived spectral index on quasars (Wilkes & Elvis 1987). But in fact, such an extrapolation is conservative; the observed X-ray/optical spectral slopes for quasars and Seyfert 1 galaxies are more typically 1.5 (Mushotzky & Wandel 1989), implying a larger amount of quasar-associated UV light. Lower luminosity AGN, including NGC4395, tend, if anything, toward slightly higher spectral indices (Lira et al. 1999). The amount of absorption along the line of sight to M33 X-8 based on our analysis of the UV/optical spectra of the nucleus and X-ray estimates of the column density of N_H of $\sim 10^{21}$ cm^{-2} to M33 X-8 itself (e.g. Long et al. 1996), and so emission from a mini-AGN would seem to be difficult to hide.

(2) Furthermore the mass contained within the M33 nucleus is simply too small to power a mini-AGN. Even a decade ago Kormendy & McClure (1993) had limited the mass of any central SMBH to $< 5 \times 10^4 M_\odot$ from the velocity dispersion of the nucleus. More recently, Lauer et al. (1998) reduced this limit to $< 2 \times 10^4 M_\odot$ with higher spatial resolution HST imagery, and most recently Gebhardt et al. (2001) lowered it further to $< 1500 M_\odot$! Hence the M33 nucleus is totally unlike the SMBH in the center of our Galaxy.

²Our inspection of the HST images of the “jet”, which was identified in V and R, indicates that it is almost certainly a small number of stars, one of which is the blue star whose spectrum we discuss here.

4.2. Or Black-Hole X-ray Binary/ULX?

Therefore, we believe that a single X-ray binary must provide the explanation for X-8. It cannot be multiple because, using data obtained over 5 years with ROSAT, we discovered a 20% modulation of the nuclear X-ray flux with a period of 106 d (Dubus et al. 1997). Assuming the L_X of $\sim 10^{39} \text{erg s}^{-1}$ is produced by an Eddington-limited source, a compact object mass of $\sim 10 M_\odot$ is required. This is in the middle of the range of dynamically-determined masses for the black-hole X-ray binaries (see, e.g. Charles 2001). If this is correct, then M33 X-8 is analogous to the large number of comparably bright (but off-nuclear) sources now being found by Chandra and XMM within nearby spirals (see, e.g. King et al. 2001), rather than an AGN nucleus.

However, the great majority of the BHXRBs have low-mass stellar donors (and hence are LMXBs) and are X-ray transient sources (see e.g. King 2000), a behavior very different from the remarkably steady (on a ~ 20 year timescale) X-ray output of M33 X-8. This suggests that the companion may be massive, in which case the source is more analogous to Cyg X-1, which is of comparable mass and not transient. Cyg X-1 also has a “superorbital” period of 142 ± 7 d, which is interpreted as precession of the disk in the system (Brocksopp et al. 1999). As a result, we suggested that the BH companion is a giant orbiting with a period of ~ 10 days and the 106 d modulation is “superorbital” (Dubus et al. 1997).

A HMXB might also be expected given the existence of a cluster of early-type stars in the M33 nucleus resulting from recent starburst activity. There would have been about 200 stars more massive than $8 M_\odot$ created in the 40 Myr starburst that exists in M33. If this picture is correct, then the location of M33 X-8 in the nucleus may be fortuitous, and of more importance is the association with recent star formation.

In this case, the history of the binary system forming M33 X-8 is more akin to the ultra-luminous X-ray sources (ULX) identified with young associations in e.g. the Antennae (Fabbiano, Zezas, & Murray 2001). However, M33 X-8 is one of the lower luminosity ULX sources, since many of them approach $\sim 10^{40} \text{erg s}^{-1}$, for which compact object masses of $\sim 100 M_\odot$ are being inferred (e.g. Makishima et al. 2000). There are several points to be made about these mass estimates, which are based upon an Eddington-limiting luminosity for a uniformly radiating source:

(1) As noted by Makishima et al. (2000) and Watarai, Mizuno, & Mineshige (2001), although multi-color disk models provide good fits to X-ray spectra of ULX sources, the disk temperatures are in the range 1.1–1.8 keV, which is much too high for $\sim 100 M_\odot$ BHs. King et al. (2001) have proposed a specific model involving mild beaming (essentially the opening cone angle of the inner accretion disc) to reduce the implied compact object mass.

(2) There are also clearly some sources that exceed the Eddington limit. For example, we already know that neutron star XRBs, such as A0538-66, the periodically recurrent transient in the LMC, are capable of reaching $\sim 10^{39}$ erg s $^{-1}$ (see e.g. Charles et al. 1983). And since this is a fast X-ray pulsar (~ 70 ms) this is presumably associated with the highly non-spherical magnetic accretion of the neutron star geometry. (We note in passing that there are several other XRBs in the LMC that are more luminous than their galactic counterparts. For example Clark et al. (1978) have suggested that this is associated with the lower metallicity of the LMC.)

The micro-quasar X-ray transient GRS 1915+105 may be the closest analogue to M33 X-8 in our Galaxy. While GRS 1915+105 is labelled as a “transient” X-ray source, it has actually been “on” now for a decade, and we believe that the few decades lifetime of X-ray astronomy is much too short to make clear-cut distinctions in the “steady/transient” label for many objects.

Early high mass estimates for the BH in GRS 1915+105 now appear to be incorrect. Greiner, Morgan, & Remillard (1998) showed with RXTE X-ray spectroscopy that this source with a peak X-ray luminosity of $\sim 7 \times 10^{39}$ erg s $^{-1}$ in the 1-200 keV band (or even greater if the lower limit for the energy band was taken down to 0.1 keV) fully qualifies as an ULX with an implied luminosity-estimated mass of order $70 M_{\odot}$. Gliozzi, Bodo, & Ghisellini (1999) pointed out that the minimum bulk kinetic power of $> 3 \times 10^{40}$ erg s $^{-1}$ during the jet ejection events far exceeded the observed peak X-ray luminosity, and hence inferred a very massive compact object as the energy source. Furthermore the observation of 67 Hz X-ray QPOs in GRS 1915+105 was interpreted as evidence for a $\sim 33 M_{\odot}$ compact object (Morgan, Remillard, & Greiner 1997). However, following their identification (Greiner et al. 2001) of the spectral type of the mass donor in GRS 1915+105, Greiner, Cuby, & McCaughrean (2001) announced the discovery of the orbital period (33.5 d) and radial velocity curve of the IR counterpart to the X-ray source. This implies a compact object mass of $14 \pm 4 M_{\odot}$, very similar to, but at the upper end of, the masses of the other BHXRBS. It should be noted that Greiner’s IR spectrum implies a low-mass ($\sim 1.2 M_{\odot}$) but evolved (K-M giant) companion, not the early-type companion that had been suggested in previous studies.

Consequently, we suggest that the properties of M33 X-8 and GRS 1915+105 can be used to draw useful comparisons with the ULX population. Based on the evidence at hand, all may be explainable as ~ 10 – $20 M_{\odot}$ BHs.

4.3. But is it possible that the O star near the nucleus is the optical counterpart?

Our bias is to associate the M33 X-8 with the nucleus of M33, rather than the O star located NNW of the nucleus. Our bias, as has been the bias of most if not all of those interested in M33 X-8, is based upon its positional coincidence with the nucleus and the fact it is so luminous compared to other sources in M33 (and the local group). The spectra we have obtained of the O star have not provided evidence that undercut our prejudices on this issue. There are a large number of late O stars spread over M33; there remains only one nucleus.

If the star were the optical counterpart, the X-ray to optical luminosity ratio of ~ 30 would be extreme for an X-ray system involving a high mass companion and therefore one might expect that the effect of the X-ray source on the companion would also be extreme. But most optical counterparts are revealed by time variations in either the broad band continuum due to heating of the companion's photosphere or to phase-dependent variations in line profiles produced by ionization of the companion's wind (see, e.g. van Loon, Kaper, & Hammerschlag-Hensberge 2001). As we noted, the spectrum of the star NNW of the nucleus appears normal for a late type O giant. But our observations were not structured for searches for orbital phase dependent effects, given typical orbital period of massive X-ray binaries, and therefore it is not possible to completely rule out the O star as the optical counterpart.

The question of where M33 X-8 is located could and should be solved using Chandra, although not with the existing CCD observations, which are saturated at the position of the nucleus (Jonathan McDowell 2001, private communication).

5. Conclusions

In summary, we have carried out the first high S/N UV and FUV spectroscopic study of the nucleus of M33. Our analysis confirms that at least two populations of stars exist in the nucleus, and that star formation occurred in the nucleus 40-50 Myrs ago. The X-ray source in the nucleus of M33 does not affect the UV spectrum significantly, all of which is consistent with the absence of a supermassive black hole or mini-quasar at the center of the nucleus, and the hypothesis that the brightest X-ray source in the Local Group is a BH with a high-mass companion. M33 X-8 will remain interesting as the nearest ULX, even though it is hidden at UV and visible wavelengths in the light of the relatively unreddened nucleus of M33.

This work was supported by NASA through grant G0-6544 from the Space Telescope Science Institute, which is operated by AURA, Inc., under NASA contract NAS5-26555. GD acknowledges additional support from NASA grants NAG5-7007 and NAG5-7034. Brian Monroe, a Data Analyst at STScI, helped us to reduce the data for this project.

REFERENCES

- Allen, C. W. 1973, *Astrophysical Quantities* (Athlone Press : London), p 204
- Brocksopp, C., Fender, R. P., Larionov, V., Lyuty, V. M., Tarasov, A. E., Pooley, G. G., Paciesas, W. S., & Roche, P. 1999, *MNRAS*, 309, 1063
- Calzetti, D., Kinney, A. L., & Storchi-Bergmann, T. 1994, *ApJ*, 429, 582
- Charles, P. 2001, *Black Holes in Binaries and Galactic Nuclei. Proceedings of the ESO Workshop held at Garching, Germany, 6-8 September 1999.* Lex Kaper, Edward P. J. van den Heuvel, Patrick A. Woudt (eds.), p. 27.
- Charles, P. A. et al. 1983, *MNRAS*, 202, 657
- Clark, G., Doxsey, R., Li, F., Jernigan, J. G., & van Paradijs, J. 1978, *ApJ*, 221, L37
- Dubus, G., Charles, P. A., Long, K. S., & Hakala, P. J. 1997, *ApJ*, 490, L47
- Dubus, G., Long, K. S., & Charles, P. A. 1999, *ApJ*, 519, L135
- Fabbiano, G., Zezas, A., & Murray, S. S. 2001, *ApJ*, 554, 1035
- Gebhardt, K. et al. 2001, *AJ*, 122, 2469
- Giozzi, M., Bodo, G., & Ghisellini, G. 1999, *MNRAS*, 303, L37
- Gordon, K. D. & Clayton, G. C. 1998, *ApJ*, 500, 816
- Gordon, K. D., Hanson, M. M., Clayton, G. C., Rieke, G. H., & Misselt, K. A. 1999, *ApJ*, 519, 165
- Greiner, J., Cuby, J. G., & McCaughrean, M. J. 2001, *Nature*, 414, 522
- Greiner, J., Cuby, J. G., McCaughrean, M. J., Castro-Tirado, A. J., & Mennickent, R. E. 2001, *A&A*, 373, L37
- Greiner, J., Morgan, E. H., & Remillard, R. A. 1998, *New Astronomy Review*, 42, 597

- King, A. R. 2000, MNRAS, 312, L39
- King, A. R., Davies, M. B., Ward, M. J., Fabbiano, G., & Elvis, M. 2001, ApJ, 552, L109
- Kormendy, J. & McClure, R. D. 1993, AJ, 105, 1793
- Koratkar, A., Deustua, S. E., Heckman, T., Filippenko, A. V., Ho, L. C., & Rao, M. 1995, ApJ, 440, 132
- Lauer, T. R., Faber, S. M., Ajhar, E. A., Grillmair, C. J., & Scowen, P. A. 1998, AJ, 116, 2263
- Leitherer, C. et al. 1999, ApJS, 123, 3
- Lira, P., Lawrence, A., O'Brien, P., Johnson, R. A., Terlevich, R., & Bannister, N. 1999, MNRAS, 305, 109
- Long, K. S., Charles, P. A., Blair, W. P., & Gordon, S. M. 1996, ApJ, 466, 750
- Long, K. S., D'Odorico, S., Charles, P. A., & Dopita, M. A. 1981, ApJ, 246, L61
- Long, K. S., & van Speybroeck, L. P. 1983, X-Ray Emission from Normal Galaxies, in Accretion Driven Stellar X-Ray Sources, ed. W. H. G. Lewin, & E. P. J. van den Heuvel (Cambridge University Press Cambridge), 117
- Makishima, K. et al. 2000, ApJ, 535, 632
- Markert, T. H. & Rallis, A. D. 1983, ApJ, 275, 571
- Massey, P., Bianchi, L., Hutchings, J. B., & Stecher, T. P. 1996, ApJ, 469, 629
- Matthews, L. D. et al. 1999, AJ, 118, 208
- Merritt, D., Ferrarese, L., & Joseph, C. L. 2001, Science, 293, 1116
- Mighell, K. J. & Rich, R. M. 1995, AJ, 110, 1649
- Minniti, D., Olszewski, E. W., & Rieke, M. 1993, ApJ, 410, L79
- Morgan, E. H., Remillard, R. A., & Greiner, J. 1997, ApJ, 482, 993
- Mushotzky, R. F. & Wandel, A. 1989, ApJ, 339, 674
- O'Connell, R. W. 1983, ApJ, 267, 80
- Schmidt, A. A., Bica, E., & Alloin, D. 1990, MNRAS, 243, 620

- Seaton, M. J. 1979, MNRAS, 187, 73P
- Supper, R., Hasinger, G., Lewin, W. H. G., Magnier, E. A., van Paradijs, J., Pietsch, W.,
Read, A. M., & Trümper, J. 2001, A&A, 373, 63
- Takano, M., Mitsuda, K., Fukazawa, Y., & Nagase, F. 1994, ApJ, 436, L47
- van den Bergh, S. 1991, PASP, 103, 609
- van Loon, J. T., Kaper, L., & Hammerschlag-Hensberge, G. 2001, A&A, 375, 498
- Walborn, N. R., Parker, J. W., & Nichols, J. S. 1995, International Ultraviolet Explorer
Atlas of B-type spectra from 1200 to 1900 Å, NASA Reference Publication, 1363
- Walborn, N. R., Nichols-Bohlin, J. & Panek, R. 1995, International Ultraviolet Explorer Atlas
of O-Type Spectra from 1200 - 1900 Å, NASA Reference Publication, 1155
- Watarai, K., Mizuno, T., & Mineshige, S. 2001, ApJ, 549, L77
- Wilkes, B. J. & Elvis, M. 1987, ApJ, 323, 243
- Woodgate, B. E. et al. 1998, PASP, 110, 1183

Fig. 1.— The flux-calibrated spectrum of the nucleus of M33. The more prominent absorption lines are labelled and the positions of the Balmer lines are indicated.

Fig. 2.— The flux-calibrated spectrum of the star NNW of the nucleus M33. The stronger stellar and interstellar features are labelled. Note that the vertical scales differ in the three panels.

Fig. 3.— A comparison between the spectrum of the nucleus and the “best-fitting” single component models. In the upper panel, the best-fit assuming a starburst absorption law is offset above the data. The best fit assuming a Galactic absorption law is plotted below the data. The lower panel shows the difference between the best-fitting single component model with a starburst absorption law and the data.

Fig. 4.— A comparison between the spectrum of the nucleus and the “best-fitting” two component normal abundance synthesis model. The higher resolution UV spectra were interpolated into the model spectra in the fits shown here. A starburst reddening curve was assumed for the M33 nucleus; the associated $E(B-V)$ of the best-fit was 0.06. The contribution of the 50 Myr and 1 Gyr bursts of star formation are also shown in the upper panel. The difference spectrum (model-data), shown in the bottom panel shows evidence of a 2200 Å feature.

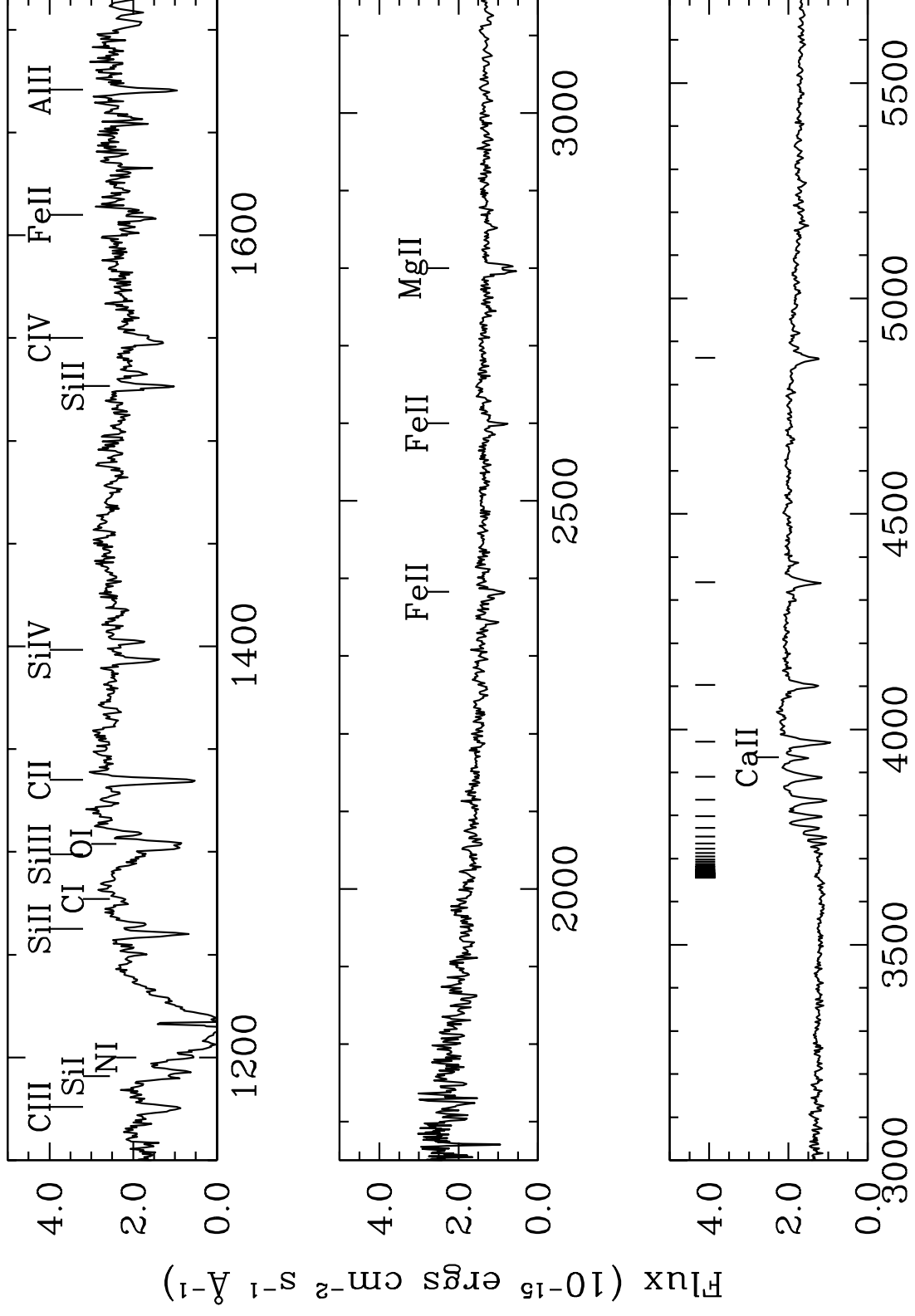
Fig. 5.— A comparison between the spectrum of the nucleus and the “best-fitting” two component normal abundance synthesis model, when allowing for a fixed Galactic extinction of $E(B-V)=0.07$ and separate M33 absorption parameterized in terms of a starburst reddening curve. The contributions of the 40 Myr and 1 Gyr starbursts are also shown in the upper panel. The fitted reddening associated with M33 corresponds to an $E(B-V)=0.11$. The difference spectrum in the lower panel indicates there are no significant departures between the data and the model including Galactic absorption that cannot be accounted for by the limited resolution of the model spectra or interstellar lines.

Fig. 6.— A comparison between the UV spectrum star NNW of the nucleus M33 compared to the O9 II template from the atlas used by Leitherer et al. (1999).

Table 1. Journal of HST STIS Observations of M33 Nucleus

Observation Date	Detector	Grating	Wavelength Range (Å)	Exposure (s)
1999-Oct-06	FUV-MAMA	G140L	1150-1736	10,157
2000-Oct-20	NUV-MAMA	G230L	1570-3180	2,810
2000-Oct-20	CCD	G430L	2900-5700	2,128

M33 Nucleus



Wavelength(\AA)

